**NASA TECHNICAL NOTE**

NASA TN D-3813

# INTERPRETATION OF (d,α) REACTIONS
# ON FLUORINE 19 AND NITROGEN 15

*by Joseph R. Priest and John S. Vincent*

*Lewis Research Center*

*Cleveland, Ohio*

NATIONAL AERONAUTICS AND SPACE ADMINISTRATION • WASHINGTON, D. C. • APRIL 1967

NASA TN D-3813

# INTERPRETATION OF (d,α) REACTIONS ON

# FLUORINE 19 AND NITROGEN 15

By Joseph R. Priest and John S. Vincent

Lewis Research Center
Cleveland, Ohio

NATIONAL AERONAUTICS AND SPACE ADMINISTRATION

# INTERPRETATION OF (d, α) REACTIONS ON FLUORINE 19 AND NITROGEN 15

by Joseph R. Priest* and John S. Vincent

Lewis Research Center

## SUMMARY

The angular distributions of five alpha-particle groups from $F^{19}(d, \alpha)O^{17}$ and $N^{15}(d, \alpha)C^{13}$ were measured. These reactions are alpha-particle emitting reactions from deuterons incident upon fluorine 19 and nitrogen 15 leaving oxygen 17 and carbon 13, respectively, as the residual nuclei. The ground and first two excited states of oxygen 17 and the ground and first excited state of carbon 13 were resolved. The nominal deuteron energy was 20.9 MeV in the laboratory system. The distorted-wave Born approximation calculation for a direct-interaction mechanism provided an adequate interpretation of the reactions. The differential cross sections integrated from $20^O$ to $170^O$ were not proportional to $2I + 1$ ($I$ is the angular momentum quantum number of the residual state). This was interpreted to be a consequence of a direct-interaction mechanism rather than of a compound-nucleus mechanism.

## INTRODUCTION

$F^{19}(d, \alpha)O^{17}$, the alpha-particle emitting reaction from deuterons incident upon fluorine 19 which results in formation of the ground and low-lying states of oxygen 17, has been investigated for several energies between 5.5 and 14.7 MeV (refs. 1 to 4). All angular distributions exhibited an oscillatory structure with some large-angle peaking that decreased as the deuteron energy increased. These data were analyzed primarily by assuming a two-nucleon pickup mechanism and by using either a plane-wave or a distorted-wave Born approximation (DWBA) calculation. Satisfactory agreement with experiment has been obtained in only a few isolated cases. The integrated differential cross sections showed an approximately smooth decrease as the deuteron energy increased. At 9.2 MeV (ref. 3) there was some correlation between the integrated cross sections and $2I + 1$ (referred to as the $2I + 1$ rule), where $I$ is the spin quantum number of a state in the re-

_____
*Associate Professor of Physics, Miami University, Oxford, Ohio.

sidual nucleus. Energy-dependence trends in these data indicated that the reaction mechanism may simplify as the deuteron energy increases. In addition, the behavior of the $2I + 1$ rule for larger deuteron energies is important. If it is valid, irrespective of the deuteron energy, this rule provides a method of determining the spin quantum number of a state in the residual nucleus.

The ground and first excited states of $O^{17}$ and the ground state of carbon 13 are well-defined single-particle states. However, both the second excited of $O^{17}$ and the first excited state of $C^{13}$ require excitation of a particle from the core nucleus (or for $C^{13}$ an inversion of the $1s_{1/2}$ and $1d_{5/2}$ shell model states) to account for the parity of the states. Therefore, some correlation might be expected between the magnitudes and shapes of the angular distributions and the character of the residual states. For these reasons, the differential cross sections corresponding to the production of the ground and first excited states of $C^{13}$ were measured for $N^{15}(d, \alpha)C^{13}$, the alpha-particle emitting reaction from deuterons incident upon nitrogen 15 leaving $C^{13}$ as the residual nucleus.

## SYMBOLS

| | |
|---|---|
| a | diffuseness parameter |
| $E_d$ | deuteron energy |
| I | spin quantum number of residual state in nucleus |
| $J_f$ | angular-momentum of residual nucleus |
| $J_i$ | angular momentum of target nucleus |
| L | angular-momentum transfer, in units of $\hbar$ |
| $l_d$ | orbital angular momentum of bound deuteron |
| $l_\alpha$ | orbital angular momentum of bound alpha particle |
| $Q_0$ | ground state reaction Q-value |
| $Q_1$ | first excited state reaction Q-Value |
| $Q_2$ | second excited state reaction Q-Value |
| R | radius of optical form factor |
| $S_d$ | intrinsic angular momentum of deuteron |
| $S_\alpha$ | intrinsic angular momentum of alpha particle |
| V | real part of complex optical potential |
| W | imaginary part of optical potential |
| $\alpha_i$ | alpha particle, which corresponds to excitation of $i^{th}$ state in residual nucleus |

2

| $\theta_{cm}$ | center-of-mass reaction angle |
|---|---|
| $\Sigma$ | summation over reaction angles |
| $\sigma$ | center-of-mass differential cross section, $\mu b/sr$ |
| $d\sigma/d\Omega$ | differential cross sections |
| $\Delta\sigma$ | statistical uncertainty in differential cross section |
| $\chi^2$ | chi-squares function |
| $\alpha, \beta, \gamma$ | constants used to normalize theoretical calculations to experimental results |

Subscripts:

| DWBA | distorted-wave Born approximation |
|---|---|
| exp | experimental |
| th | theoretical |

# PROCEDURE

The experimental detection and particle discrimination were the same as in a previous $(d, \alpha)$ experiment (ref. 5). The $F^{19}$ targets used were 1.43 milligrams per square centimeter commercial films[1] of Teflon $(CF_2)$. The targets deteriorated rapidly because of the deuteron bombardment and had to be changed periodically. A fixed-monitor counter, which recorded deutrons elastically scattered from the $CF_2$ target, reflected this target deterioration and also provided a method for correcting the data for different target thicknesses. The internal consistency of the data indicates the appropriateness of this procedure. Typical spectra of alpha particles are shown for $F^{19}(d, \alpha)O^{17}$ reactions (fig. 1(a)) and for $N^{15}(d, \alpha)C^{13}$ reactions (fig. 1(b)).

Nitrogen 15 gas with a purity of 99 percent (obtained from Isomet Corp., 433 Commercial Ave., Palisades Park, N. J.) was used for the $N^{15}(d, \alpha)C^{13}$ experiment. It was contained in a cylindrical gas cell $4\frac{3}{4}$ inches in diameter and $\frac{3}{4}$ inch thick. The walls of the cell were covered with Havar foil 0.0001 inch thick. (Havar is a cobalt-base high-strength alloy manufactured by the Hamilton Watch Company, Lancaster, Pennsylvania.) The pressure was measured with a resistance-type strain-gage transducer to an accuracy of 0.05 millimeter of mercury. The nominal pressure of the gas was 14.5 centimeters of mercury. The ambient temperature of the gas was measured to an accuracy of $0.5^O$ K with an iron-constantan thermocouple using an ice-water mixture for a reference temperature.

---

[1]These films were manufactured by the Dilectrix Corporation, Farmingham, Long Island, and were donated by Professor O. E. Johnson, Purdue University, Lafayette, Indiana.

# EXPERIMENTAL RESULTS AND OBSERVATIONS

The experimental results of this study are presented in tables I and II. The experimental and theoretical results are plotted in the form of center-of-mass differential cross section ($\mu$b/sr) against center-of-mass reaction angle (deg)(figs. 2 to 4). The origin of the theoretical curves is discussed in the next section.

The most striking features of these results are (1) the distinct oscillatory behavior of the angular distribution corresponding to production of the 0.871 MeV first excited state of $O^{17}$ (fig. 2) and the ground state of $C^{13}$ (fig. 4(a)), and (2) the lack of enhancement of the $F^{19}(d, \alpha)O^{17}$ differential cross sections for large angles. This second feature was not observed for a deuteron energy of 9.2 MeV (ref. 3). The well-defined structure of the angular distributions indicates that, perhaps, only a single reaction mechanism predominates and, therfore, the theoretical interpretation may be simplified.

# DISCUSSION

## DWBA Analysis of Reactions

$\underline{F^{19}(d, \alpha)O^{17} \text{ reaction.}}$ - In the simplest theoretical formalism, a $(d, \alpha)$ reaction proceeds by a pickup and/or knockout direct-interaction mechanism. In the pickup model, a neutron-proton pair is picked up from the target nucleus to form an alpha particle. In the knockout model, the target is depicted as a core plus an alpha particle, which is knocked out by the incident deuteron. The residual nucleus then consists of the core plus the captured deuteron. In light nuclei, where the shell-model description of the nucleus is usually adequate, the pickup mechanism is preferred. However, present simple direct-interaction theories cannot distinguish the mechanisms on the basis of the angular distributions. Therefore, since a working computer code (ref. 6) that utilizes the DWBA formalism (ref. 7) for knockout reactions was available, it was chosen for the analysis of the results of this study.

The DWBA calculation utilizes wave functions that are determined from optical-model elastic-scattering calculations for the incident deuteron and exit alpha-particle channels. There is, however, no experimental information on ($F^{19}$ + d) or ($O^{17}$ + $\alpha$) at the appropriate energies. Consequently, several analyses of experimental data for low charge-number nuclei near $F^{19}$ and $O^{17}$ were examined (ref. 8). Although there are ambiguities in the optical-model parameters for a given nucleus, a given set of parameters is reasonably appropriate for several nuclei for the same bombarding energy. Therefore, a typical set was chosen, namely, V, W, a, and R (table III). These parame-

ters are the same as those of the Woods-Saxon potential, which is defined as

$$- \left[ V + iW \right] \left[ 1 + \exp\left( \frac{r - R}{a} \right) \right]^{-1}$$

The spin-orbit term in the optical potential is ignored because the available computer code did not incorporate this term in the DWBA calculation. These parameters were fixed throughout the calculations. Only the cutoff radius was varied. The meaning of the cutoff radius is discussed later in this section (p. 12).

The angular-momentum transfer $\vec{L}$ for knockout reactions is defined from the equation

$$\vec{J}_f = \vec{J}_i + \vec{S}_d + \vec{l}_d - \vec{l}_\alpha \tag{1}$$

$$= \vec{J}_i + \vec{S}_d + \vec{L} \tag{2}$$

which imply that $\vec{L} = \vec{l}_d - \vec{l}_\alpha$, since $S_\alpha = 0$. If the parities of the initial and final states are the same, L is an even integer, and if the parities differ, L is an odd integer. This selection rule limits the possible values of L. The ground-state spin and parity of $F^{19}$ is $1/2^+$. By using this and the known spins and parities of the appropriate states of $O^{17}$, the allowed values of L were determined and are given in table IV.

Because of the apparent simplicity of the results for production of the 0.871-MeV state of $O^{17}$, these results were analyzed first to obtain the proper cutoff radius parameter. Although both $L = 0$ and $L = 2$ are allowed, the shape (ref. 8) of the angular distribution indicates that $L = 0$ is preferred. The DWBA calculation that uses a cutoff radius of 4.58 fermis is shown in figure 2. Since the normalization of the theoretical calculation is somewhat arbitrary, it is worthwhile to explain the method that was used. A standard procedure is to match the theoretical and experimental curves at the first maximum in the angular distribution. Normally the shapes are reasonably similar only in the angular region around the first maximum. This is not the case for the data presented herein. Therefore, the procedure chosen was one which determined the normalizing constant $\alpha$ that minimized the chi-squares function $\chi^2$.

$$\chi^2 = \sum_\theta \left[ \frac{\alpha \sigma_{th}(\theta) - \sigma_{exp}(\theta)}{\Delta\sigma_{exp}} \right]^2 \tag{3}$$

where $\Delta\sigma_{exp}$ is the statistical uncertainty in the differential cross section. The theoretical curve shown in figure 2(a) was normalized in this fashion. It can be seen that the agreement with experiment is quite satisfactory over the entire angular range studied. The main difference is that the experimental minimums are shallower than those predicted by theory. It is presumptuous, however, to expect exceptional agreement without having included the contributions of the $L = 2$ transition and the spin-orbit term in the optical potential. The $L = 2$ contribution was determined in the following manner: the DWBA calculation was performed by assuming the same optical-model parameters and cutoff radius as for the $L = 0$ calculation. The $L = 0$ and $L = 2$ incoherent contributions were then obtained by determining the normalizing constants $\beta$ and $\gamma$, which minimized the chi-squares function defined by

$$\chi^2 = \sum_{\theta} \left[ \frac{\beta\sigma_0(\theta) + \gamma\sigma_2(\theta) - \sigma_{exp}(\theta)}{\Delta\sigma_{exp}} \right]^2 \tag{4}$$

The result of adding 11 percent of the $L = 2$ component is shown in figure 2(b). The agreement with experiment is not exceptionally better than that obtained by using only the $L = 0$ contribution (fig. 2(a)), but it is more realistic in the sense that there is much better agreement at the minimums.

The same DWBA parameters were used to calculate the differential cross sections for production of the ground state of $O^{17}$. For this reaction, $L = 2$ and $L = 4$ are allowed. The incoherent contributions were then determined by using equation (4), and the results are shown in figure 3(a). The agreement with experiment is not as good as that obtained for production of the first excited state. Nevertheless, the theoretical curve is acceptable and does reproduce the general character of the experimental results. Better agreement can be obtained by varying the DWBA parameters slightly. However, if the theoretical calculations are of any significance, the same parameters should be used throughout.

The second excited state of $O^{17}$ has spin 1/2 and odd parity. Thus, only $L = 1$ is allowed. The character of this state differs from the ground and first excited states because the single-particle shell model requires excitation of a nucleon from the $O^{16}$ core to form this negative parity state. The smaller differential cross sections for production of this state (fig. 3(b)) seem to confirm this. To obtain the theoretical curve shown in figure 3(b), the cutoff radius parameter was increased slightly to 4.93 fermis. This increase was not unjust because of the different character of this state. These data were normalized by using equation (3). Again, the agreement with experiment is not exact but it is acceptable.

In the DWBA formalism using the cutoff radius approach, all contributions to the scattering amplitude for a radial distance less than the cutoff radius are neglected. Although this is not a physical assumption, it has yielded good agreement with experiment in many reactions such as deuteron stripping. This success has not been so pronounced in $(d, \alpha)$ reactions. Recently Buck and Rook (ref. 9) examined this cutoff radius DWBA theory in some detail and concluded that if the theory adequately characterizes the experimental results, the cutoff radius should be about 1 fermi greater than the nuclear radius. If it is assumed that the nuclear radius is $r_0 A^{1/3}$, where A is the mass number and $r_0$ is 1.25 fermis, the radius of the $F^{19}$ nucleus is 3.33 fermis. The cutoff radius used was 4.58 fermis, which tends to confirm Buck's supposition.

$N^{15}(d, \alpha)C^{13}$ reaction. - The ground-state spin and parity of both $N^{15}$ and $C^{13}$ is $1/2^-$. In the shell model description, this is attributed to the odd $1p_{1/2}$ proton in $N^{15}$ and to the odd $1p_{1/2}$ neutron in $C^{13}$. The first excited state of $C^{13}$ also has spin 1/2 but has even parity. This state is not as easily understood from the shell model. If it is assumed that $C^{13}$ is a $C^{12}$ core plus a neutron, then this state requires excitation of a particle from the core or an inversion of the $1s_{1/2}$ and $1d_{5/2}$ shell model states. This is tantamount to the situation in the $F^{19}(d, \alpha)O^{17}$ reaction. Based on results of that reaction, it is anticipated that the transition to the first excited state of $C^{13}$ will be inhibited. A comparison of figures 4(a) and (b) shows this to be the case. The first excited state was so weakly excited that only a partial angular distribution was obtained. The differential cross sections, which correspond to excitation of this state, are, in general smaller by a factor of more than 2 than those corresponding to the ground-state transitions.

The method of selecting optical-model parameters for the DWBA analysis of these data was the same as for the $F^{19}$ data. The radius parameters for the deuteron and alpha-particle channels were reduced from the values in table III to 3.80 and 4.26 fermis, respectively, to account for the smaller radii of the $N^{15}$ and $C^{13}$ nuclei. For the ground-state transition, both L = 0 and L = 2 are allowed. The results for L = 2 with a cutoff radius of 3.30 fermis are shown in figure 4(a). The L = 2 calculation gave a substantially better fit than the L = 0 calculation. Although the L = 2 fit is not strikingly good, it is judged to be satisfactory. An incoherent mixture of the L = 0 calculation gave no significant improvement in the fit. Fischer and Fischer (ref. 10) who studied this reaction by using a more simplified treatment, also concluded that L = 2 gave the best overall fit. Since only a partial angular distribution was obtained for the first excited-state transition, no detailed analysis was made for these data. The cutoff radius of 3.30 fermis used for the $N^{15}$ reaction is closer to the nuclear radius of $N^{15}$ than was the case for the $F^{19}$ analysis.

## Integrated Cross Sections and 2I + 1 Rule

In several (d, α) reactions, the integrated differential cross sections if averaged over a range of bombarding energies were proportional to 2I + 1 (refs. 3 and 11 to 13). The energy range interval must be sufficient to eliminate any special correlation between the compound and final states. A few hundred kilovolts are usually adequate. In the data reported herein and in many experiments elsewhere, the energy spread due to finite target thickness and cyclotron beam is sufficient to produce the necessary energy interval.

The differential cross sections for the data presented herein were integrated from $20^\circ$ to $170^\circ$ (fig. 5). In addition, some data for the $5/2^-$ and $3/2^-$ third and fourth excited states are presented. However, the angular distributions for these states were of poor quality because of counting statistics and inadequate energy resolution. Clearly the 2I + 1 rule is not obeyed for this reaction at this energy.

In a theoretical study of the 2I + 1 rule, MacDonald (ref. 14) and Ericson (ref. 15) listed certain criteria to be satisfied in order to validate the 2I + 1 rule. Foremost of these is that a compound nucleus reaction mechanism be involved. The general character of the angular distributions and the adequate interpretation within the DWBA formalism indicate that this reaction mechanism does not favor the formation of a compound nucleus. Thus the stipulation that the reactions proceed by a compound nucleus mechanism appears to be necessary for the validity of the 2I + 1 rule. The remaining criteria appear to be satisfied in the experiment reported herein.

It is interesting that the integrated cross sections for production of the even-parity single-particle states are proportional to 2I + 1, as are the integrated cross sections for excitation of the odd-parity excited-core states. Although these results are based on limited data and may be strictly fortuitous, the effect should be investigated for other (d, α) reactions.

# CONCLUDING REMARKS

The cutoff radius DWBA formalism for (d, α) knockout reactions has provided an adequate description of the $F^{19}(d, \alpha)O^{17}$ and $N^{15}(d, \alpha)C^{13}$ reactions at 20.9 MeV. Although this interpretation may not be unique, the good agreement with theory does provide an impetus to investigate other (d, α) reactions and theories. Transitions to residual states, which require core excitation in the shell-model description, are inhibited. Proportionality between the integrated differential cross sections for the $F^{19}(d, \alpha)O^{17}$ reaction and the 2I + 1 rule was not observed. This lack of proportionality was interpreted to be a consequence of a direct interaction mechanism rather than of a compound-nucleus

mechanism. Although the data are limited, they suggest that, if the residual states are of the same character, the $2I + 1$ rule for these states may be obeyed.

Lewis Research Center,
National Aeronautics and Space Administration,
Cleveland, Ohio, October 28, 1966,
129-02-04-06-22.

# REFERENCES

1. Hu, Chuin: $(d, \alpha)$ Reactions on Some Light Nuclei. J. Phys. Soc. Japan, vol. 15, no. 10, Oct. 1960, pp. 1741-1752.

2. Takamatsu, Kunio: $(d, \alpha)$ Reactions on $F^{19}$, $Ne^{20}$, $P^{31}$ and $S^{32}$ at 14.7 MeV. J. Phys. Soc. Japan, vol. 17, no. 6, June 1962, pp. 896-906.

3. Cosper, S. W.; Lucas, B. T.; and Johnson, O. E.: $F^{19}(d, \alpha)O^{17}$ Reaction at 9.2 MeV. Phys. Rev., vol. 138, no. 1B, Apr. 12, 1965, pp. 51-57.

4. Wesolowski, Jerome J.; Hansen, Luisa F.; Vidal, Jose G.; and Stelts, Marion L.: Two-Nucleon Distorted-Wave Born Approximation Analysis of $F^{19}(d, \alpha)O^{17}$ Data. Phys. Rev., vol. 148, no. 3, Aug. 19, 1966, pp. 1063-1071.

5. Priest, Joseph R.; and Vincent, John S.: Investigation of the $(d, \alpha)$ Reaction on Aluminum 27. NASA TN D-3548, 1966.

6. Gibbs, W. R.; Madsen, V. A.; Miller, J. A.; Tobocman, W.; Cox, E. C.; and Mowry, L.: Direct Reaction Calculation. NASA TN D-2170, 1964.

7. Tobocman, W.: Theory of Direct Nuclear Reactions. Oxford University Press, 1961.

8. Pehl, Richard H.: Studies in Nuclear Spectroscopy by Two-Nucleon Transfer Reactions. Rep. No. UCRL-10993, California Univ., Lawrence Radiation Lab., Aug. 28, 1963.

9. Buck, B.; and Rook, J. R.: Remarks on the Theory of Direct Reactions. Nucl. Phys., vol. 67, 1965, pp. 504-516.

10. Fischer, G. E.; and Fischer, V. K.: Study of $(d, \alpha)$ Reactions on Some Light Nuclei. Phys. Rev., vol. 114, no. 2, Apr. 15, 1959, pp. 533-539.

11. Hinds, S.; Middleton, R.; and Litherland, A. E.: Further Evidence for the $(2I + 1)$ Rule in the $Al^{27}(d, \alpha)Mg^{25}$ Reaction. Proceedings of the Rutherford Jubilee International Conference, Manchester, 1961. J. B. Birks, ed., Academic Press, 1961, pp. 305-306.

12. Colli, L.; Iori, I.; Marcazzan, M. G.; and Milazzo, M.: Properties of Compound Nucleus From Experimental Measurement of the $Si^{28}(n, \alpha)Mg^{25}$ Reaction. Nucl. Phys., vol. 43, 1963, pp. 529-536.

13. Hansen, O.; Koltay, E.; Lund, N.; and Madsen, B. S.: The (2I + 1) Rule Applied to the (d, $\alpha$) Reactions on $Mg^{25}$ and $Al^{27}$. Nucl. Phys., vol. 51, 1964, pp. 307-311.

14. MacDonald, N.: The (2I + 1) Rule and the Statistical Compound Nucleus Theory. Nucl. Phys., vol. 33, 1962, pp. 110-117.

15. Ericson, Torleif: Classical Theory of Compound Nucleus Reactions. Nucl. Phys., vol. 17, 1960, pp. 250-263.

TABLE I. - EXPERIMENTAL DATA FOR $F^{19}(d,\alpha)O^{17}$

| (a) Ground state; spin quantum number of residual nuclear state, $5/2^+$; reaction Q-value, 10.038 MeV | | | (b) First excited state; spin quantum number of residual nuclear state, $1/2^+$; reaction Q-value, 10.038 - 0.871 MeV | | | (c) Second excited state; spin quantum number of residual nuclear state, $1/2^-$; reaction Q-value, 10.038 - 3.058 MeV | | |
|---|---|---|---|---|---|---|---|---|
| Center-of-mass reaction angle, $\theta_{cm}$, deg | Differential cross section, $d\sigma/d\Omega$, $\mu$b/sr | Statistical error, $\mu$b/sr | Center-of-mass reaction angle, $\theta_{cm}$, deg | Differential cross section, $d\sigma/d\Omega$, $\mu$b/sr | Statistical error, $\mu$b/sr | Center-of-mass reaction angle, $\theta_{cm}$, deg | Differential cross section, $d\sigma/d\Omega$, $\mu$b/sr | Statistical error, $\mu$b/sr |
| 16.9 | 482.1 | 10.3 | 16.9 | 20.4 | 2.1 | 17.0 | 22.0 | 2.2 |
| 19.7 | 341.3 | 12.8 | 19.7 | 29.7 | 3.8 | 19.8 | 14.3 | 2.6 |
| 22.5 | 306.8 | 8.2 | 22.5 | 45.8 | 3.2 | 22.6 | 19.1 | 2.0 |
| 25.3 | 193.0 | 9.7 | 25.3 | 41.1 | 4.5 | 25.5 | 13.9 | 2.6 |
| 28.1 | 165.2 | 6.1 | 28.1 | 68.4 | 3.9 | 28.3 | 13.0 | 1.7 |
| 30.9 | 107.7 | 4.3 | 31.0 | 57.8 | 3.5 | 31.1 | 12.1 | 2.4 |
| 33.7 | 91.3 | 3.2 | 33.7 | 55.4 | 2.5 | 33.9 | 10.2 | 1.3 |
| 36.5 | 76.5 | 4.0 | 36.5 | 40.6 | 2.9 | 36.7 | 8.9 | .7 |
| 39.2 | 77.5 | 3.3 | 39.3 | 28.0 | 2.0 | 31.1 | 11.9 | 2.0 |
| 42.0 | 70.7 | 5.1 | 42.1 | 17.7 | 2.5 | 39.4 | 12.6 | 1.3 |
| 44.7 | 70.3 | 3.1 | 44.8 | 15.6 | 1.5 | 42.2 | 13.3 | 2.2 |
| 47.5 | 72.1 | 5.1 | 47.6 | 22.0 | 2.8 | 45.0 | 14.2 | 1.4 |
| 50.2 | 66.4 | 3.1 | 50.3 | 29.1 | 2.0 | 47.8 | 15.7 | 2.4 |
| 52.9 | 61.7 | 4.9 | 53.0 | 36.7 | 3.7 | 50.5 | 8.2 | 1.1 |
| 55.6 | 42.2 | 1.9 | 55.7 | 31.5 | 1.7 | 53.2 | 4.2 | 1.3 |
| 58.3 | 35.8 | 3.7 | 58.4 | 27.6 | 3.3 | 55.9 | 2.8 | 0.5 |
| 61.0 | 31.7 | 2.0 | 61.1 | 21.4 | 1.6 | 58.7 | 1.9 | .9 |
| 63.7 | 36.1 | 3.8 | 63.8 | 22.6 | 3.0 | 61.4 | 3.0 | .6 |
| 66.4 | 30.6 | 2.0 | 66.5 | 11.4 | 1.0 | 64.1 | 5.1 | 1.4 |
| 69.0 | 34.7 | 3.7 | 69.1 | 6.5 | 1.6 | 66.7 | 5.2 | .7 |
| 71.7 | 28.8 | 1.7 | 71.8 | 6.2 | 0.8 | 69.4 | 7.2 | 1.7 |
| 76.9 | 32.1 | 3.5 | 77.0 | 13.7 | 2.3 | 72.0 | 5.6 | .7 |
| 82.1 | 33.9 | 3.6 | 82.2 | 21.8 | 2.9 | 77.3 | 4.9 | 1.4 |
| 87.2 | 38.3 | 3.3 | 87.3 | 29.0 | 2.9 | 82.5 | .78 | .55 |
| 89.8 | 34.5 | 1.8 | 89.9 | 25.1 | 1.5 | 87.7 | 1.7 | .7 |

| | | | | | | | | |
|---|---|---|---|---|---|---|---|---|
| 92.3 | 31.8 | 3.1 | 92.4 | 22.0 | 2.6 | 90.2 | 1.9 | 0.4 |
| 94.8 | 26.7 | 1.6 | 94.9 | 17.9 | 1.3 | 92.7 | 3.0 | .9 |
| 97.3 | 29.2 | 3.0 | 97.5 | 12.8 | 2.0 | 95.3 | 5.2 | .7 |
| 99.8 | 26.0 | 1.3 | 99.9 | 8.7 | .9 | 97.8 | 3.0 | 1.0 |
| 102.3 | 20.8 | 2.5 | 102.4 | 5.6 | 1.3 | 100.3 | 3.7 | .5 |
| 104.8 | 27.7 | 1.3 | 104.9 | 4.5 | 0.5 | 102.7 | 2.8 | 0.9 |
| 107.2 | 24.5 | 2.7 | 107.3 | 4.5 | 1.2 | 105.2 | 3.6 | .5 |
| 109.7 | 25.4 | 2.2 | 109.8 | 6.3 | .8 | 107.6 | 2.4 | .8 |
| 112.1 | 33.3 | 3.2 | 112.2 | 8.6 | 1.6 | 110.1 | 6.4 | .9 |
| 114.5 | 28.1 | 1.8 | 114.6 | 12.2 | 1.2 | 112.5 | 2.8 | .9 |
| 116.9 | 26.2 | 2.9 | 117.0 | 10.6 | 1.8 | 117.3 | 4.1 | 1.1 |
| 119.3 | 23.5 | 1.5 | 119.4 | 12.9 | 1.2 | 119.7 | 3.4 | .8 |
| 121.6 | 21.4 | 2.6 | 121.7 | 13.7 | 2.1 | 122.0 | 3.9 | 1.1 |
| 124.0 | 22.4 | 1.5 | 124.1 | 7.2 | .9 | 124.4 | 2.9 | .7 |
| 126.3 | 16.0 | 1.8 | 126.4 | 8.5 | 1.3 | 126.7 | 1.8 | .6 |
| 128.7 | 16.5 | 1.7 | 128.8 | 8.1 | 1.2 | 129.0 | 3.0 | 0.7 |
| 131.0 | 16.9 | 1.2 | 131.1 | 6.1 | .7 | 131.3 | 1.7 | .6 |
| 133.3 | 18.8 | 1.9 | 133.4 | 5.8 | 1.0 | 133.6 | 2.6 | .7 |
| 135.6 | 21.6 | 1.4 | 135.7 | 4.8 | .6 | 135.9 | 1.6 | .4 |
| 137.9 | 25.8 | 2.5 | 138.0 | 5.8 | 1.2 | 138.2 | 2.0 | .7 |
| 140.2 | 25.1 | 1.5 | 140.3 | 3.5 | 0.6 | 140.5 | 0.87 | 0.43 |
| 142.4 | 31.6 | 2.8 | 142.5 | 3.3 | .9 | 142.7 | 1.8 | .7 |
| 144.7 | 31.4 | 1.7 | 144.8 | 4.8 | .7 | 145.0 | 1.2 | .5 |
| 146.9 | 35.4 | 3.0 | 147.0 | 3.4 | .9 | 147.2 | 1.3 | .6 |
| 149.2 | 27.4 | 1.7 | 149.3 | 8.4 | 1.0 | 149.4 | 1.4 | .6 |
| 151.4 | 31.7 | 2.9 | 151.5 | 2.4 | 0.8 | 151.6 | 2.1 | 0.8 |
| 153.7 | 27.6 | 1.8 | 153.7 | 8.3 | 1.0 | 153.8 | 2.2 | .7 |
| 155.9 | 27.8 | 2.6 | 158.1 | 10.8 | 1.1 | 156.0 | 2.4 | .8 |
| 158.1 | 27.9 | 1.8 | 155.9 | 11.4 | 1.7 | 158.2 | 5.1 | 1.1 |
| 160.3 | 35.5 | 2.9 | 160.3 | 15.9 | 2.0 | 160.4 | 3.9 | 1.0 |
| 162.5 | 31.5 | 2.6 | 162.5 | 13.9 | 1.8 | 164.8 | 5.9 | 1.2 |
| 164.7 | 41.8 | 3.2 | 164.7 | 13.3 | 1.8 | 169.1 | 4.7 | 1.1 |
| 169.1 | 56.9 | 3.7 | 169.1 | 17.3 | 2.1 | | | |

# TABLE II. - EXPERIMENTAL DATA FOR $N^{15}(d, \alpha)C^{13}$

(a) Ground state; spin quantum number of residual nuclear state, $1/2^-$; reaction Q-value 7.687 MeV

(b) First excited state; spin quantum number of residual nuclear state, $1/2^+$; reaction energy, 7.687 - 3.09 MeV

| Center-of-mass reaction angle, $\theta_{cm}$, deg | Differential cross section, $d\sigma/d\Omega$, $\mu b/sr$ | Statistical error, $\mu b/sr$ | Center-of-mass reaction angle, $\theta_{cm}$, deg | Differential cross section, $d\sigma/d\Omega$, $\mu b/sr$ | Statistical error, $\mu b/sr$ |
|---|---|---|---|---|---|
| 17.5 | 378.7 | 32.1 | 23.6 | 16.5 | 3.1 |
| 20.4 | 378.3 | 28.4 | 26.5 | 11.9 | 1.7 |
| 23.3 | 344.9 | 35.4 | 29.4 | 7.1 | 2.2 |
| 26.2 | 233.4 | 25.3 | 32.3 | 7.1 | 1.5 |
| 29.1 | 204.0 | 30.4 | 35.2 | 8.5 | 1.4 |
| 32.0 | 134.1 | 21.2 | 38.1 | 13.0 | 2.1 |
| 34.9 | 93.8 | 5.4 | 41.0 | 13.3 | 1.9 |
| 37.8 | 47.5 | 13.7 | 43.9 | 35.1 | 3.8 |
| 40.6 | 59.6 | 4.8 | 46.7 | 25.3 | 3.3 |
| 46.3 | 46.6 | 4.5 | 49.6 | 37.3 | 4.1 |
| 49.1 | 37.4 | 4.2 | 52.4 | 37.4 | 4.2 |
| 51.9 | 42.5 | 4.6 | 55.2 | 37.0 | 4.3 |
| 54.7 | 46.9 | 3.4 | 58.0 | 36.5 | 3.4 |
| 57.5 | 68.6 | 4.7 | 60.8 | 35.2 | 4.4 |
| 60.3 | 104.4 | 5.4 | 63.6 | 33.6 | 3.4 |
| 63.0 | 122.5 | 6.6 | 66.3 | 35.3 | 4.6 |
| 65.8 | 122.6 | 6.1 | 69.1 | 33.4 | 3.6 |
| 68.5 | 121.2 | 6.8 | 74.5 | 22.5 | 3.0 |
| 71.2 | 71.6 | 6.8 | 77.2 | 19.7 | 3.7 |
| 73.9 | 91.0 | 6.1 | 82.5 | 19.4 | 3.8 |
| 76.6 | 60.8 | 6.6 | 87.7 | 16.5 | 3.6 |
| 81.9 | 39.0 | 5.4 | 92.9 | 9.9 | 2.9 |
| 87.1 | 32.4 | 5.1 | 98.0 | 12.5 | 2.3 |
| 92.2 | 66.1 | 7.4 | 103.0 | 22.8 | 2.6 |
| 97.3 | 87.1 | 6.1 | 107.9 | 23.9 | 2.7 |
| 102.3 | 63.4 | 4.3 | 112.7 | 15.7 | 3.8 |
| 107.2 | 43.1 | 3.6 | | | |
| 112.1 | 21.4 | 2.6 | | | |

TABLE III. - OPTICAL MODEL PARAMETERS USED IN DISTORTED-WAVE

BORN APPROXIMATION CALCULATION

| Channel | Real part of optical potential, V, MeV | Imaginary part of optical potential, W, MeV | Diffuseness parameter, a, F | Radius of optical form factor, R, F |
|---|---|---|---|---|
| Incident deuteron | 55 | 11 | 0.65 | 3.95 |
| Exit alpha particle | 33 | 9 | .5 | 4.54 |

TABLE IV. - LEVEL PARAMETERS FOR OXYGEN 17 AND

AND ALLOWED L VALUES FOR $F^{19}(d, \alpha)O^{17}$

| Excitation energy of $O^{17}$ | Angular-momentum quantum number, $J_f$ | Parity | Allowed values of angular-momentum transfer, L |
|---|---|---|---|
| 0 | 5/2 | + | 2, 4 |
| 0.871 | 1/2 | + | 0, 2 |
| 3.058 | 1/2 | − | 1 |

(a) $F^{19}(d, \alpha)O^{17}$ reaction.
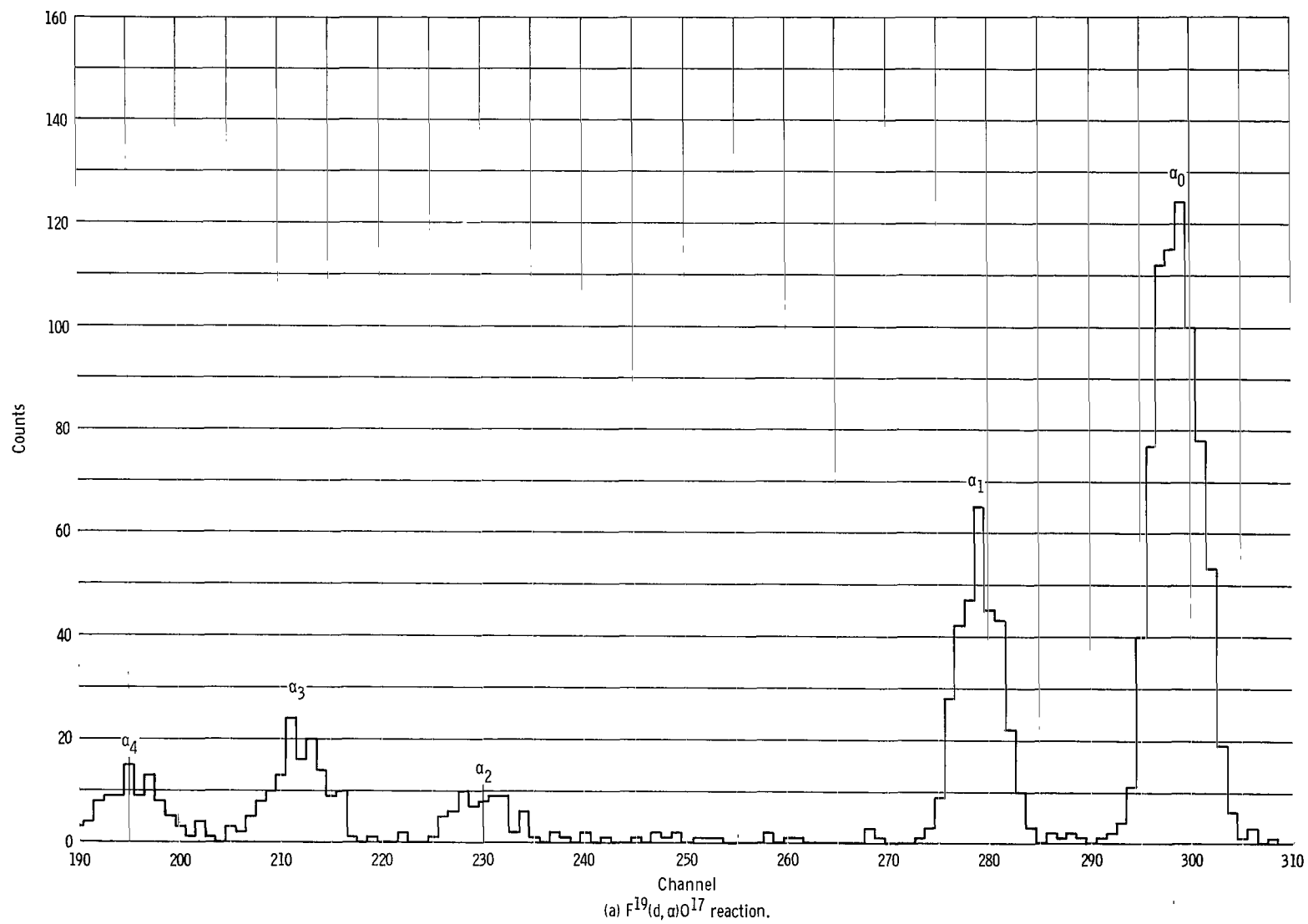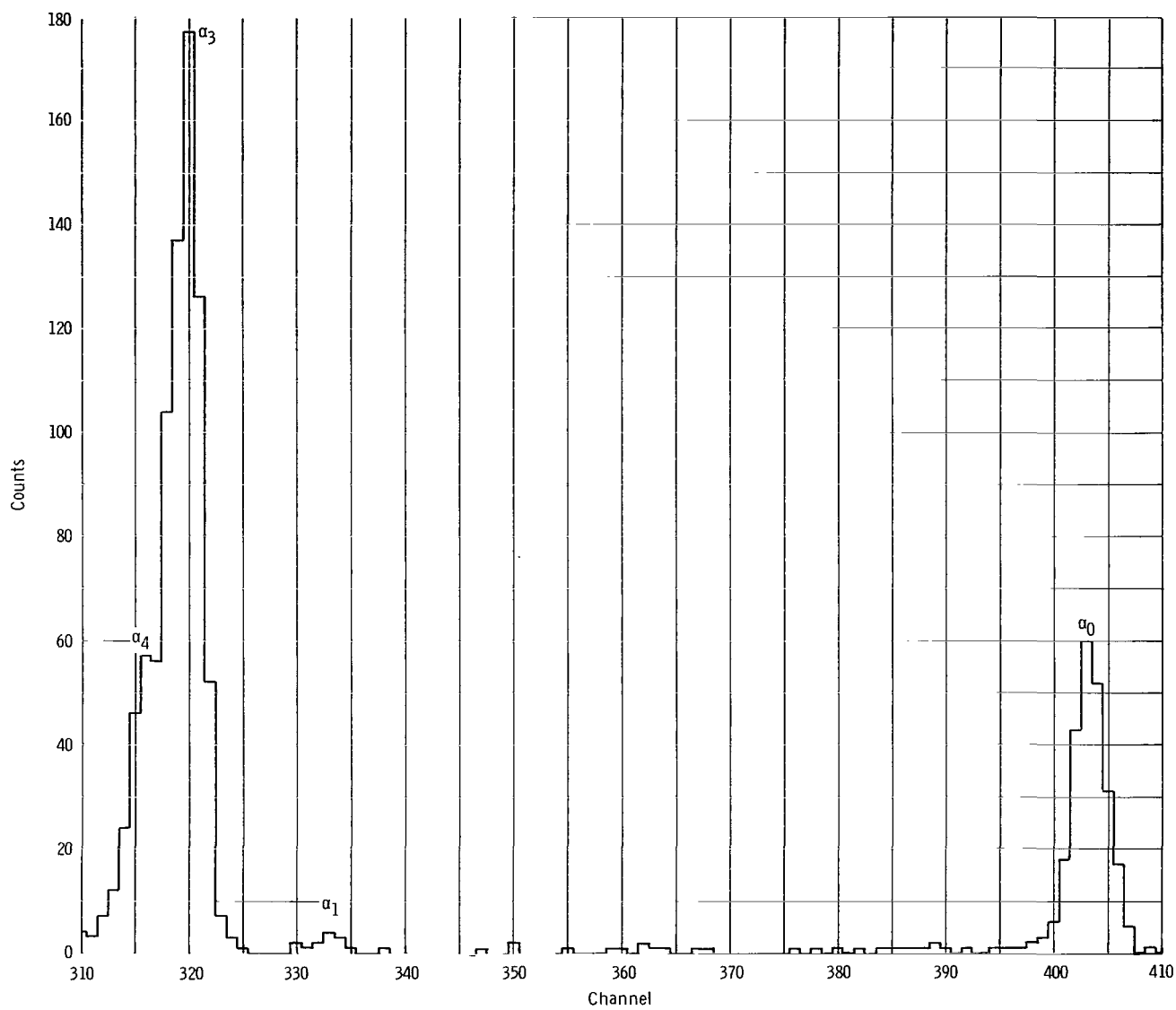
Figure 1. – Typical alpha-particle spectra for laboratory angle of 25°.

(b) $N^{15}(d, \alpha)C^{13}$ reaction.

Figure 1. - Concluded.

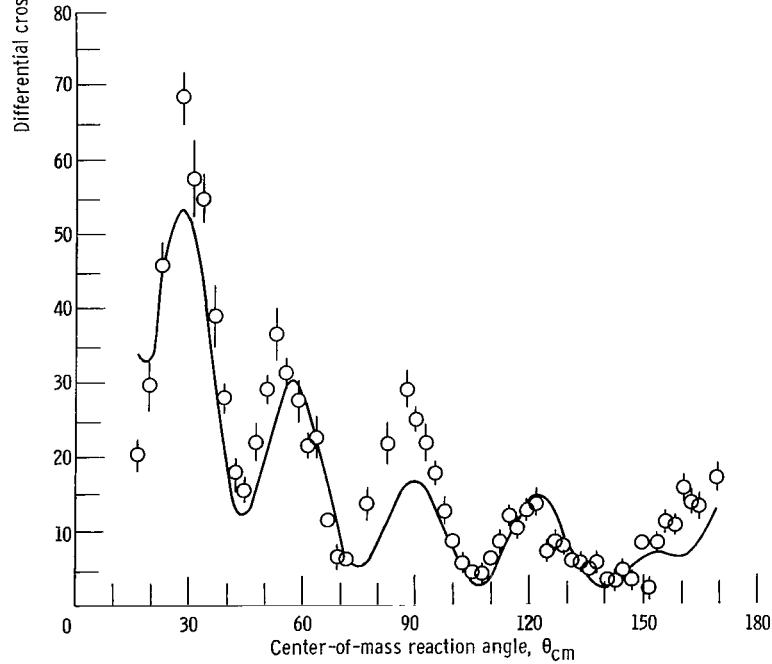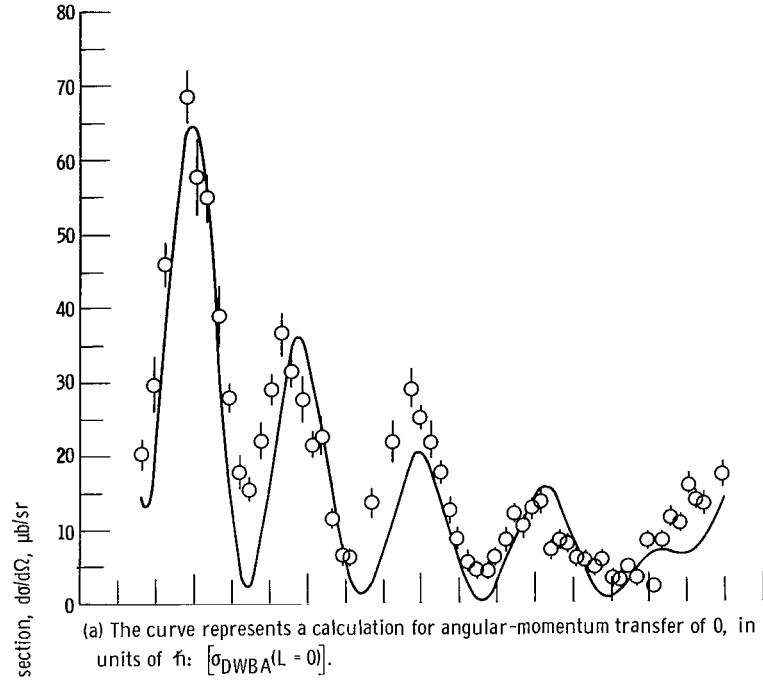(a) The curve represents a calculation for angular-momentum transfer of 0, in units of $\hbar$: $\left[\sigma_{DWBA}^{(L\ =\ 0)}\right]$.

(b) The curve represents a calculation for a mixture of cross sections for angular-momentum transfers of 0 and 2, in units of $\hbar$: $\left[\sigma_{DWBA}^{(L\ =\ 0)}\right.$ $+\ 0.11\ \left.\sigma_{DWBA}^{(L\ =\ 2)}\right]$.

Figure 2. - Comparison of differential cross sections for reaction $F^{19}(d,\alpha)O^{17}$, first excited state, with prediction of distorted-wave Born approximation. Reaction Q-value, 10.038 - 0.871 MeV; deuteron energy, 20.9 MeV; spin quantum number, $1/2^{+}$ for initial and final state.
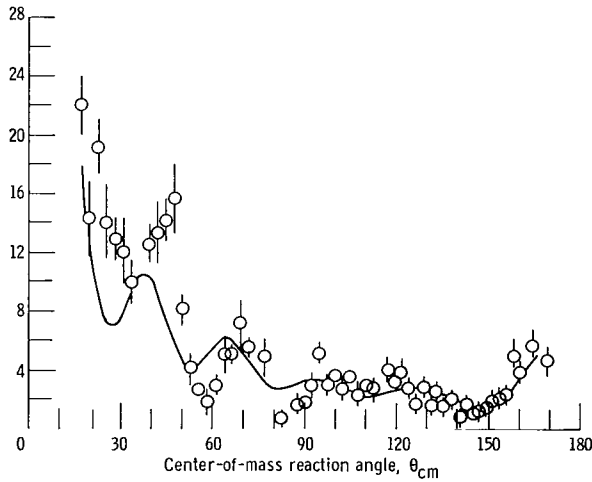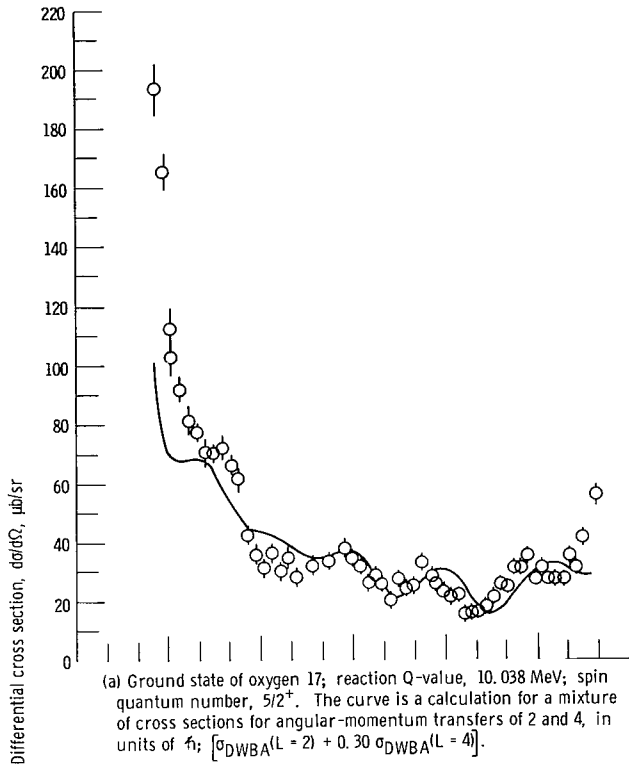
18

(a) Ground state of oxygen 17; reaction Q-value, 10.038 MeV; spin quantum number, $5/2^+$. The curve is a calculation for a mixture of cross sections for angular-momentum transfers of 2 and 4, in units of $\hbar$: $\left[\sigma_{DWBA}^{(L=2)} + 0.30\ \sigma_{DWBA}^{(L=4)}\right]$.

(b) Second excited state of oxygen 17; reaction Q-value, $10.038 - 3.058$ MeV; spin quantum number, $1/2^-$. The curve is a calculation for angular-momentum transfer of 1, in units of $\hbar$: $\left[\sigma_{DWBA}^{(L=1)}\right]$.

Figure 3. – Comparison of differential cross sections for $F^{19}(d,\alpha)O^{17}$ with prediction of distorted-wave Born approximation. Deuteron energy, 20.9 MeV; spin quantum number of fluorine 19, $1/2^+$.
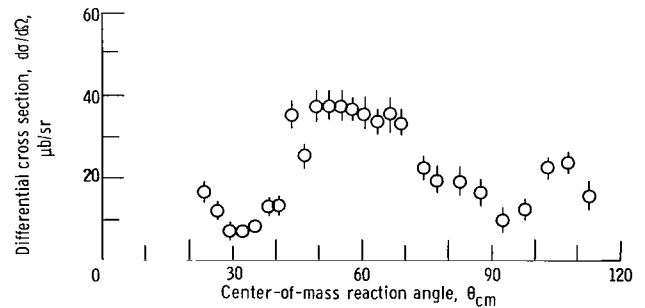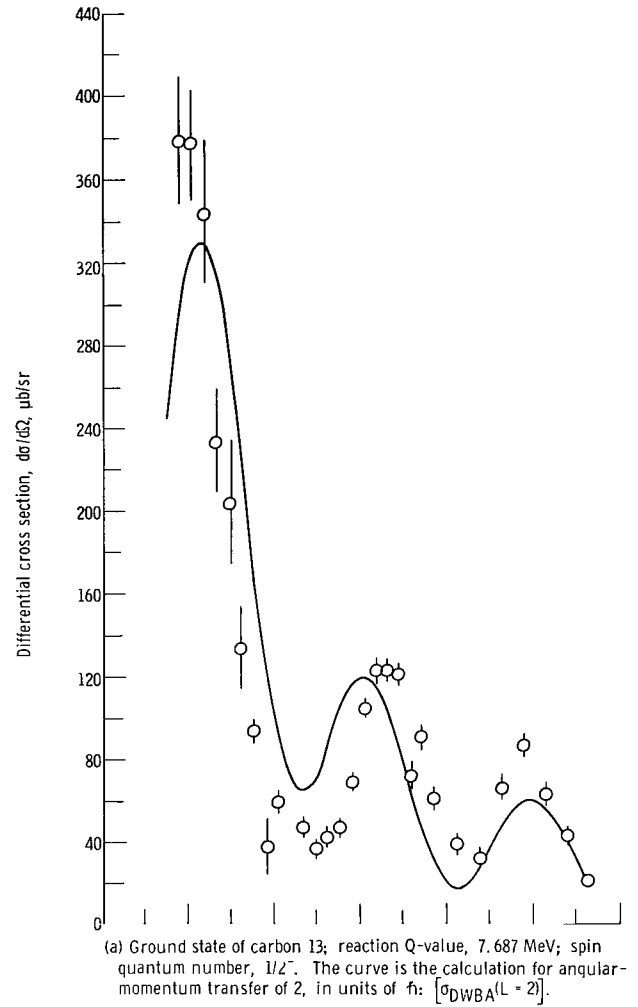
(a) Ground state of carbon 13; reaction Q-value, 7.687 MeV; spin quantum number, $1/2^-$. The curve is the calculation for angular-momentum transfer of 2, in units of $\hbar$: $\left[\sigma_{DWBA}^{(L=2)}\right]$.

(b) First excited state of carbon 13; reaction Q-value, $7.687 - 3.09$ MeV; spin quantum number, $1/2^+$.

Figure 4. – Differential cross sections for $N^{15}(d,\alpha)C^{13}$. Deuteron energy, 20.9 MeV; spin quantum number for nitrogen 15, $1/2^-$.
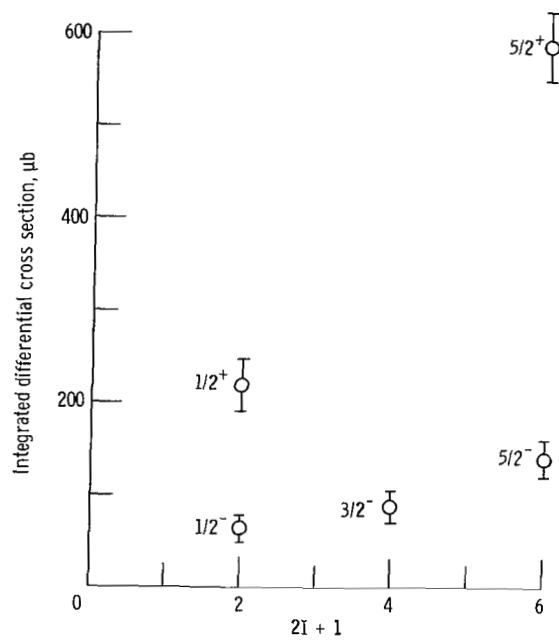
19

Figure 5. – Differential cross sections for $F^{19}(d, \alpha)O^{17}$ reactions integrated from $20°$ to $170°$.

*"The aeronautical and space activities of the United States shall be conducted so as to contribute . . . to the expansion of human knowledge of phenomena in the atmosphere and space. The Administration shall provide for the widest practicable and appropriate dissemination of information concerning its activities and the results thereof."*

—NATIONAL AERONAUTICS AND SPACE ACT OF 1958

# NASA SCIENTIFIC AND TECHNICAL PUBLICATIONS

TECHNICAL REPORTS: Scientific and technical information considered important, complete, and a lasting contribution to existing knowledge.

TECHNICAL NOTES: Information less broad in scope but nevertheless of importance as a contribution to existing knowledge.

TECHNICAL MEMORANDUMS: Information receiving limited distribution because of preliminary data, security classification, or other reasons.

CONTRACTOR REPORTS: Scientific and technical information generated under a NASA contract or grant and considered an important contribution to existing knowledge.

TECHNICAL TRANSLATIONS: Information published in a foreign language considered to merit NASA distribution in English.

SPECIAL PUBLICATIONS: Information derived from or of value to NASA activities. Publications include conference proceedings, monographs, data compilations, handbooks, sourcebooks, and special bibliographies.

TECHNOLOGY UTILIZATION PUBLICATIONS: Information on technology used by NASA that may be of particular interest in commercial and other non-aerospace applications. Publications include Tech Briefs, Technology Utilization Reports and Notes, and Technology Surveys.

*Details on the availability of these publications may be obtained from:*

SCIENTIFIC AND TECHNICAL INFORMATION DIVISION

# NATIONAL AERONAUTICS AND SPACE ADMINISTRATION

Washington, D.C. 20546